Surrealistic Bohm Trajectories

Berthold-Georg Englert[1,2], Marlan O. Scully[3], Georg Süssmann, and Herbert Walther[1,2]

[1] Sektion Physik, Universität München, Am Coulombwall 1, D-8046 Garching, Germany
[2] Max-Planck-Institut für Quantenoptik, Ludwig-Prandtl-Straße 10, W-8046 Garching.
[3] Department of Physics, Texas A & M University, College Station, TX 77843-4242.

Z. Naturforsch. **47a**, 1175–1186 (1992); received September 22, 1992

A study of interferometers with one-bit which-way detectors demonstrates that the trajectories, which David Bohm invented in his attempt at a *realistic* interpretation of quantum mechanics, are in fact *surrealistic*, because they may be macroscopically at variance with the observed track of the particle. We consider a two-slit interferometer and an incomplete Stern-Gerlach interferometer, and propose an experimentum crucis based on the latter.

Introduction

In Bohmian mechanics [1–3], ordinary quantum theory [4] is supplemented by classical particle trajectories. These trajectories are usually unobserved – indeed, they are unobservable in the face of Heisenberg's uncertainty relation for position and momentum – but nevertheless they are regarded as realistic, similar to the tracks seen in a bubble chamber. Yes, such tracks supposedly exhibit Bohm trajectories within the limitations set by uncertainty relations. More common, however, is the situation in which a particle is detected without being observed earlier, and then the particle's Bohm trajectory can be *retro*dicted. This retrodiction assigns reality to the Bohm trajectories in an operational sense, the more so because the actual trajectory cannot be *pre*dicted owing to the fundamental ignorance of the actual initial position. Predictions in Bohmian mechanics are limited by the probabilistic knowledge about initial conditions, which knowledge comes from quantal probability distributions. Therefore, the predictive power of Bohmian mechanics does not exceed that of ordinary quantum theory, and so the alleged superiority of Bohmian mechanics over ordinary quantum theory is of a purely philosophical nature.

A particle traverses a bubble chamber and is then detected. Does the retrodicted Bohm trajectory always agree with the observed track? Our answer is: No. For, our considerations show that the Bohm trajectory may be macroscopically at variance with the recorded track. For the sake of simplicity, we do, however, not study the complicated motion of a charged particle through a bubble chamber, where many degrees of freedom are involved. Instead, we look at atom interferometers, and a few which-way detectors replacing the plethora of bubbles. These one-bit which-way detectors are placed such that they enable us to distinguish one class of tracks from another, macroscopically different one. It turns out that the atom's Bohm trajectory may not belong to the observed class of tracks. We are thus led to the conclusion that the Bohm trajectories, originally introduced with the aim of arriving at a "realistic interpretation" of quantum theory, are in fact surrealistic.

The next section contains a concise review of Bohmian mechanics. Then we turn to gedanken experiments in which atoms pass through double slits, eventually supplemented by which-way detectors capable of recording through which slit the atom went without thereby disturbing the atom's center-of-mass motion. We find that there are events when the Bohm trajectory goes through one slit, but the atom through the other. This is followed by a detailed treatment of magnetic atoms traversing an incomplete Stern-Gerlach interferometer. Here the track recorded by the which-way detectors is *always* macroscopically different from the corresponding Bohm trajectories. We are thus proposing an experimentum crucis which, according to our quantum theoretical prediction, will clearly demonstrate that the reality attributed to Bohm trajectories is rather metaphysical than physical.

In Appendix A we supply a brief description of quantum-optical which-way detectors, which have been discussed in detail elsewhere [5].

Reprint requests to Prof. Dr. G. Süssmann, Sektion Physik, Universität München, Am Coulombwall 1, W-8046 Garching bei München.

0932-0784 / 92 / 1200-1175 $ 01.30/0. – Please order a reprint rather than making your own copy.

The one-bit which-way detectors may evolve dynamically in Bohmian mechanics, too. The description is then changed quantitatively but not qualitatively. A large fraction of atomic Bohm trajectories remains macroscopically at variance with the recorded track. This situation is discussed in Appendix B.

Bohmian Mechanics in a Nutshell

In Bohmian mechanics [1–3] the continuity equation

$$\frac{\partial}{\partial t}\varrho(t,\boldsymbol{r}) + \nabla\cdot\boldsymbol{j}(t,\boldsymbol{r}) = 0\,, \tag{1}$$

obeyed by the probability density ϱ for finding the particle in the vicinity of the point $\boldsymbol{r}$ and the corresponding probability current density $\boldsymbol{j}$, is taken as the starting point for defining, and eventually computing, trajectories $\boldsymbol{R}(t)$. These Bohm trajectories are interpreted as the possible paths along which the particle could have propagated. The actual trajectory is then selected by the (initial or rather) final position that is somehow observed. The trajectories are determined by Bohm's velocity field $\boldsymbol{v}(t,\boldsymbol{r})$ that is given by

$$\boldsymbol{v}(t,\boldsymbol{r}) = \boldsymbol{j}(t,\boldsymbol{r})/\varrho(t,\boldsymbol{r})\,. \tag{2}$$

Fortunately, knowledge of $\boldsymbol{v}$ where $\varrho = 0$ is never needed. The differential equation

$$\frac{\mathrm{d}}{\mathrm{d}t}\boldsymbol{R}(t) = \boldsymbol{v}(t,\boldsymbol{R}(t)) \tag{3}$$

in conjunction with a known position at some instant – usually when the particle is finally detected – then supplies the actual Bohm trajectory. The probabilistic predictions of ordinary quantum theory remain unaltered because an ensemble of trajectories that mimicks ϱ at one time will equally well mimick ϱ at any later time. So, with the understanding that in repeated experiments initial positions are realized according to the probabilities implied by ϱ, an ensemble average over the corresponding trajectories will agree with the quantum theoretical predictions. In addition, before the velocity field (2) is available, one must first solve the Schrödinger equation for the underlying wave function from which ϱ and $\boldsymbol{j}$ are then calculated. Thus, the Bohm trajectories cannot provide us with more information than what is carried by the wave function.

In the sequel we shall confine the discussion to nonrelativistic situations involving one particle of mass m. The dynamics will by governed by a Hamilton operator of the form

$$\mathbf{H} = \frac{1}{2m}\boldsymbol{p}^2 + V(\boldsymbol{t},\boldsymbol{r};\mathbf{A})\,, \tag{4}$$

where $\boldsymbol{r}$ and $\boldsymbol{p}$ are the position and momentum operators and $\mathbf{A}$ symbolizes additional degrees of freedom like spin. The wave function may then posses a number of components $\psi_\alpha(t,\boldsymbol{r})$ labelled by a subscript α. From these, ϱ and $\boldsymbol{j}$ are constructed in the familiar way:

$$\varrho(t,\boldsymbol{r}) = \sum_\alpha |\psi_\alpha(t,\boldsymbol{r})|^2\,, \tag{5}$$

$$\boldsymbol{j}(t,\boldsymbol{r}) = \frac{1}{m}\,\mathrm{Re}\sum_\alpha \psi_\alpha^*(t,\boldsymbol{r})\,\frac{\hbar}{i}\,\nabla\psi_\alpha(t,\boldsymbol{r})\,,$$

of which the latter applies only if the $\boldsymbol{p}$-dependence of $\mathbf{H}$ does not differ from that in (4).

In Bohmian mechanics, a particle has a position and nothing else, as is particularly emphasized in Bell's [6] formulation (see also [7]). The properties associated with $\mathbf{A}$ in (4) (or the label α in (5)), such like spin, are possessed and carried by the wave function only. Nevertheless, after the trajectory $\boldsymbol{R}(t)$ has been found, the values of the $\psi_\alpha(t,\boldsymbol{R}(t))$ can be employed to specify what – in a conscious departure from standard Bohmian mechanics – could be regarded as the actual values of the quantities $\mathbf{A}$. For example, if $\psi_\pm$ are the two spin-$\frac{1}{2}$ components referring to the z direction, then the unit spin vector at time t is

$$\boldsymbol{S}(t) = \frac{1}{\varrho}\begin{pmatrix} 2\,\mathrm{Re}\,\psi_+^*\,\psi_- \\ 2\,\mathrm{Im}\,\psi_+^*\,\psi_- \\ |\psi_+|^2 - |\psi_-|^2 \end{pmatrix} \tag{6}$$

with $\varrho = |\psi_+|^2 + |\psi_-|^2$ (see (5)), where $\psi_\pm$ are evaluated at $\boldsymbol{r} = \boldsymbol{R}(t)$.

Double-Silt Interferometer

Consider the symmetric double-slit set-up in Figure 1. The particles coming in from the left all have the same velocity perpendicular to the slit plate. Thus the incident wave function is a plane wave with the planes parallel to the slit plate. In the interference region between the slit plate and the screen, the wave function is the coherent superposition of the two contributions from the slits,

$$\psi(t,\boldsymbol{r}) = \psi_>(t,\boldsymbol{r}) + \psi_<(t,\boldsymbol{r})\,. \tag{7}$$

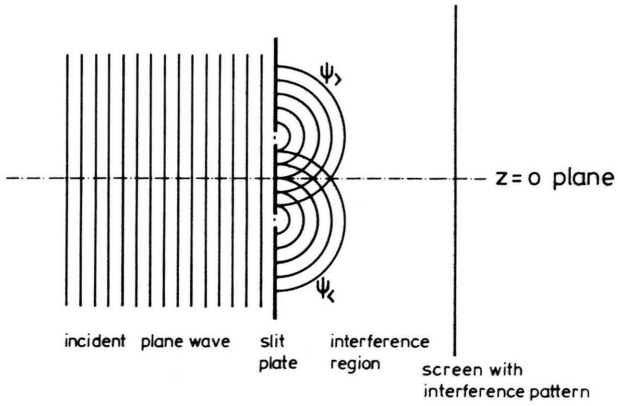

Fig. 1. Double-slit interferometer with indication of phase fronts for incident plane wave and scattered partial waves $\psi_>$ and $\psi_<$ which interfere.

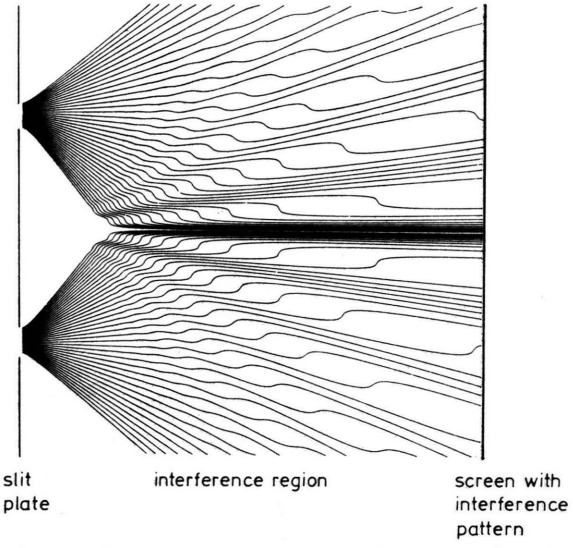

Fig. 2. Bohm trajectories in the interference region of a double-slit interferometer; adapted from [8].

In view of the geometrical symmetry of the arrangement, $\psi_<$ is obtained from $\psi_>$ by reflection at the $z=0$ plane,

$$\psi_<(t, x, y, z) = \psi_>(t, x, y, -z)\,. \tag{8}$$

Consequently, the probability density $\varrho = |\psi|^2$ as well as the x- and y-components of the current vector $\boldsymbol{j} = \frac{1}{m}\,\mathrm{Re}\,\psi^* \frac{\hbar}{i}\nabla\psi$ are even functions of z, in contrast to the z-component of $\boldsymbol{j}$, which is odd. Therefore, the z-component of the velocity field (2) is also an odd

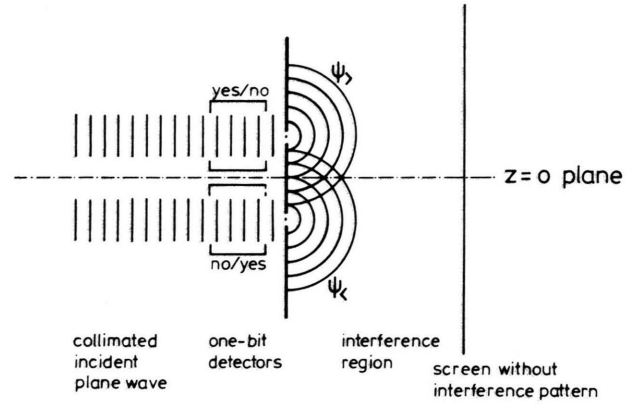

Fig. 3. Double-slit interferometer with one-bit detectors through which the collimated incident plane wave reaches the slit plate. With which-way information available, the screen no longer displays the double-slit interference pattern.

function of z, so that this component vanishes on the $z=0$ plane of symmetry. This has the immediate implication that the Bohm trajectories do not cross the $z=0$ plane [6]. In other words, when a particle has hit the upper half of the screen (where $z>0$), then its retrodicted Bohm trajectory goes through the upper slit, and those particles arriving on the lower half of the screen (where $z<0$) have, according to Bohmian mechanics, passed through the lower slit. These symmetry considerations are confirmed by the Bohm trajectories computed by Philippidis, Dewdney, and Hiley [8], see Figure 2.

In ordinary quantum mechanics, the statement that the particle went through one slit and not the other is, of course, utterly meaningless, as long as no corresponding observation is performed (as exemplified by the string of bubbles in a bubble chamber). Quite consciously, no definite classical history is assigned to a single event. An adherent of Bohmian mechanics, however, would proudly announce that he does not have to give up the concept of a classical particle trajectory when studying quantal phenomena. And really, what is the argument about? The particle is not *observed* while it traverses the apparatus in Figure 1. So why can't we all accept the Bohm trajectories as real, their empirical reality originating in retrodiction rather than direct observation?

The advanced techniques of modern quantum optics enable the experimenter to build one-bit detectors sensitive to the passage of a single atom. For a description consult Appendix A. The details of the detection mechanism are not relevant for the present discus-

sions, so we shall symbolize the one-bit recording as a transition from "no" to "yes". It is important to realize that this transition happens with virtual certainty and that the atom's center-of-mass wave function is not altered noticeably in the process.

The set-up of Fig. 1 is now supplemented by two such one-bit detectors, one for each slit as in Figure 3. The detectors will supply us with which-way information, not quite in the detailed sense of registering a whole track (like that seen in a bubble chamber), but by clearly distinguishing the class of tracks through one slit from the class through the other. The two-slit interference pattern on the screen is lost, of course, as soon as we have this which-way information available, but that is not the issue here.

With the one-bit which-way detectors in place, the wave function in the interference region is now

$$\Psi = \psi_> |^{\text{yes}}_{\text{no}}\rangle + \psi_< |^{\text{no}}_{\text{yes}}\rangle , \tag{9}$$

in which the contribution of the upper slit is correlated to the which-way information documented in the upper detector, and likewise for the lower slit *and the lower detector*. In contrast to (7), the functions $\psi_>$ and $\psi_<$ in (9) are components of the two-component wave function Ψ. The density ϱ and current $\boldsymbol{j}$ associated with Ψ are, therefore, different from what is obtained from (8). In particular, the terms responsible for the two-slit interference pattern are absent now, as it must be. However, most important for the matter of interest, the symmetry properties of ϱ and $\boldsymbol{j}$ under reflections at the $z=0$ plane are the same as before: ϱ as well as the x- and y-component of $\boldsymbol{j}$ and $\boldsymbol{v}$ are unaffected by the transformation $z \to -z$, whereas the z-components of $\boldsymbol{j}$ and $\boldsymbol{v}$ change sign and accordingly vanish on the symmetry plane $z=0$. Thus it is still true that when the atom is found on the upper half of the screen its retrodicted Bohm trajectory goes through the upper slit, and the trajectory of an atom found on the lower half passes through the lower slit.

But through which slit did the atom come? Suppose that the upper detector says "yes", the lower "no". Then the probability for finding the atom somewhere on the screen is proportional to $|\psi_>|^2$, which does *not* vanish on the lower half of the screen. Consequently, there will be events when the *atom goes through* the upper detector and therefore through *the upper slit* and then hits the lower half of the screen, so that the corresponding *Bohm trajectory goes through the lower slit*. In other words: the Bohm trajectory is here macroscopically at variance with the actual, that is: observed, track. Tersely: Bohm trajectories are not realistic, they are surrealistic.

As a result of these considerations we disagree with Bell [6] who says (words adapted to the present discussion): "The naive classical picture [of ordinary quantum mechanics] has the particle, arriving on a given half of the screen, going through the wrong slit." Per definition, the "right slit" is, for Bell, the one traversed by the Bohm trajectory. To state it once more clearly: for us, the right slit is the one through which the atom is actually observed going, never mind the naive unobservable Bohm trajectory. And if one does not observe through which slit the atom goes, then the notion of the right or the wrong slit is meaningless.

Bell [6] has more to say about double-slit interferometers with which-way detectors. His detectors, however, are not of the one-bit type, but consist of very many particles, of which a good fraction gets macroscopically displaced. Bell considers treating these particles also according to the rules of Bohmian mechanics and arrives at the conclusion that, in effect, either $\psi_>$ or $\psi_<$ becomes irrelevant. Thereafter the symmetry argument no longer applies and the Bohm trajectory passes always through the same slit as the atom's track. Bell's reasoning does not apply to the present scheme, in which no macroscopic displacements occur until the which-way information stored in the one-bit detectors is finally read off. This reading-off is done (long) after the atom has hit the screen, so the relevant Bohm velocity field is, indeed, determined by the two-component wave function (9). There the yes/no degree of freedom of the one-bit detectors appears just as a label, like α in (5). One cannot associate continuous position variables with such discrete degrees of freedom and, therefore, they are not dynamical in Bohmian mechanics, in contrast to the motional degrees of freedom of the many particles that constitute Bell's macroscopic detector.

One could object that the yes/no label of the one-bit detector need not really refer to two orthogonal states of a spin-$\frac{1}{2}$-type degree of freedom. It could just as well indicate that some physical system – a harmonic oscillator, say – is either in its ground state ("no") or in its first excited state ("yes"). Then one does have a corresponding continuous position variable with its own Bohmian dynamics. And the Bohm velocity field for the atom no longer has a definite symmetry, it changes according to the evolution of the detector variable. Consequently, now the atom trajectory may cross the $z=0$ plane. But, as discussed in

Appendix B, there remains a considerable number of trajectories that do not pass through the same slit as the atom's track.

The one-bit detectors possess yet another essential property that is lacking in macroscopic detectors. Before they are actually read off, nothing irreversible happens. One can even erase the which-way information carefully and recover the two-slit interference pattern in the process. For details consult [9].

There is one more lesson in Bell's article, a psychological one. Namely that this tentative supporter of Bohmian mechanics very much *wants* the Bohm trajectory to pass through the same slit as the observed track of the atom. Nature, however, does not grant this favor.

Incomplete Stern-Gerlach Interferometer

The double-slit interferometer for atoms with which-way detectors is very difficult, if not impossible, to realize experimentally. We have discussed its features above mainly for pedagogical reasons which include the contact made with [6] and [8]. We now turn to the much more realistic experiments in which atoms traverse three quarters of a Stern-Gerlach interferometer, see Figure 4. The missing fourth quarter, necessary for reuniting the partial beams, is absent. Therefore, entering spin-up atoms are first deflected up, then down, and finally hit the screen well below the $z=0$ plane; conversely, spin-down atoms are first deflected down, then up, and hit the screen well above the $z=0$ plane. We emphasize that both the intermediate and final separation between the beams are macroscopic and, in particular, large compared with the individual beam widths.

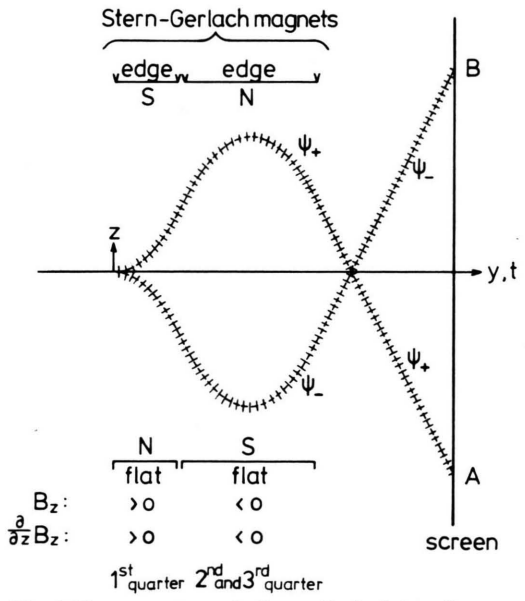

Fig. 4. Three quarters of a Stern-Gerlach interferometer. The dashed curves represent $\pm\Delta z$ of (15) along which the centers of the wave function components $\psi_\pm$ propagate. After crossing the $z=0$ plane, atoms arrive on the screen either in region A ("spin up") or in region B ("spin down").

The subtleties studied in [10], which are essential for the coherent reunion of the two partial beams in a complete (four quarters) Stern-Gerlach interferometer, are irrelevant here. We can, therefore, adopt the strategy of [11] and disregard the x-motion totally while regarding the y-motion as classical. Then y is replaced by vt and the spatial y-dependence of the magnetic field is thereby effectively turned into a time-dependence. For the z-motion and the spin evolution we then have, as in [1], the Hamilton operator

$$\mathbf{H} = \frac{1}{2m}\mathbf{p}^2 + \mathscr{E}(t)\,\sigma_z - F(t)\,z\,\sigma_z\,, \tag{10}$$

which has the structure (4) with **A** standing for the spin vector operator. The term $\mathscr{E}(t)\,\sigma_z$ is the magnetic energy at the center of the magnets (where $z=0$) and $F(t)\,\sigma_z$ is the force produced by the z-inhomogeneity of the magnetic field.

The net momentum transferred to a spin-up atom is

$$\Delta p(t) = \int_0^t \mathrm{d}t'\,F(t')\,, \tag{11}$$

and its accumulated z-displacement becomes

$$\Delta z(t) = \int_0^t \mathrm{d}t'\,\Delta p(t')/m = \int_0^t \mathrm{d}t'\,\frac{t-t'}{m}\,F(t')\,, \tag{12}$$

where $t=0$ is the instant when the atom enters the magnetic field. For example, the idealized force

$$F(t) = \begin{cases} F_0 & \text{for} \quad 0<t<T_0\,, \\ -F_0 & \text{for} \quad T_0<t<3\,T_0\,, \\ 0 & \text{for} \quad 3\,T_0<t\,, \end{cases} \tag{13}$$

where T_0 is the time to traverse one of the three quarters, yields

$$\Delta p(t) = \begin{cases} F_0\,t & \text{for} \quad 0<t<T_0\,, \\ F_0(2\,T_0-t) & \text{for} \quad T_0<t<3\,T_0\,, \\ -F_0\,T_0 & \text{for} \quad 3\,T_0<t \end{cases} \tag{14}$$

and

$$\Delta z(t) = \frac{F_0}{2m} \begin{cases} t^2 & \text{for } 0 < t < T_0, \\ 2T_0^2 - (t-2T_0)^2 & \text{for } T_0 < t < 3T_0, \\ (7T_0 - 2t)T_0 & \text{for } 3T_0 < t. \end{cases} \tag{15}$$

Hence the up and down beams intersect around time $t = \frac{7}{2} T_0$. At time $t = 2T_0$ the (macroscopic) distance between the two beams is $2|\Delta z(2T_0)| = 2F_0 T_0^2/m$, and if the position of the screen corresponds to $t = 5T_0$, the spots produced by the spin-up and spin-down atoms are $2|\Delta z(5T_0)| = 3F_0 T_0^2/m$ apart.

At the initial time $t=0$ the magnetic atom is supposed to be in a minimum uncertainty state. (This is an innocuous simplifying assumption; in an atomic beam minimum uncertainty states are hard to come by.) To take advantage of the symmetry of the set-up, we take the atom initially polarized in the x-direction and choose the spatial wave function symmetric to the $z=0$ plane. Thus the two components referring to the eigenvalues $\sigma_z = \pm 1$ of the spin operator σ_z are initially

$$\psi_+(0, z) = \psi_-(0, z) \tag{16}$$
$$= (2\pi)^{-1/4} (2\delta z_0)^{-1/2} \exp\left[-\left(\frac{z}{2\delta z_0}\right)^2\right],$$

where δz_0 is the initial spread in z, which uncertainty is small compared to the maximal separation of the beams. The corresponding spread in momentum is $\delta p = \frac{1}{2}\hbar/\delta z_0$. In a reasonable experiment one must avoid that the natural spreading happens too fast. In the present context this requires that the characteristic time $m\delta z_0/\delta p$ is at most of the order of T_0.

At later times we get, by solving the Schrödinger equation,

$$\psi_\pm(t, z) = (2\pi)^{-1/4} \left[2\left(\delta z_0 + i\frac{t}{m}\delta p\right)\right]^{-1/2} \tag{17}$$
$$\cdot \exp\left[-\frac{1}{4}\frac{(z \mp \Delta z(t))^2}{\delta z_0(\delta z_0 + i t\,\delta p/m)} \pm \frac{i}{\hbar} z\,\Delta p(t) \mp \frac{i}{2}\Phi(t)\right]$$

up to an irrelevant common z-independent phase factor. The quantity

$$\Phi(t) = \frac{2}{\hbar}\int_0^t \mathrm{d}t'\, \mathscr{E}(t') \tag{18}$$

is the accumulated Larmor precession angle. It equals

$$\Phi(t) = \begin{cases} \Omega t & \text{for } 0 < t < T_0, \\ \Omega(2T_0 - t) & \text{for } T_0 < t < 3T_0, \\ -\Omega T_0 & \text{for } 3T_0 < t \end{cases} \tag{19}$$

in the case of

$$\mathscr{E}(t) = \begin{cases} \frac{\hbar}{2}\Omega & \text{for } 0 < t < T_0, \\ -\frac{\hbar}{2}\Omega & \text{for } T_0 < t < 3T_0, \\ 0 & \text{for } 3T_0 < t. \end{cases} \tag{20}$$

The two components (17) interchange under the spatial reflection according to

$$\psi_+(t, z) = \psi_-(t, -z), \tag{21}$$

which is the essential symmetry also possessed by the components $\psi_<$ and $\psi_>$ in (9). Consequently, the probability density

$$\varrho(t, z) = |\psi_+(t, z)|^2 + |\psi_-(t, z)|^2 \tag{22}$$

and the z-component

$$j(t, z) = \frac{1}{m}\,\mathrm{Re}\left[\psi_+^* \frac{\hbar}{i}\frac{\partial}{\partial z}\psi_+ + \psi_-^* \frac{\hbar}{i}\frac{\partial}{\partial z}\psi_-\right](t, z) \tag{23}$$

of the current are symmetric and antisymmetric, respectively:

$$\varrho(t, -z) = \varrho(t, z), \quad j(t, -z) = -j(t, z). \tag{24}$$

The resulting Bohm velocity field (z-component again) is then antisymmetric, too,

$$v(t, z) = t\,z\left(\frac{\delta p}{m\,\delta z(t)}\right)^2$$
$$+\left[\frac{\Delta p(t)}{m} - t\,\Delta z(t)\left(\frac{\delta p}{m\,\delta z(t)}\right)^2\right]\tanh\left(\frac{z\,\Delta z(t)}{(\delta z(t))^2}\right)$$
$$= -v(t, -z). \tag{25}$$

Thus it vanishes on the $z=0$ plane with the now familiar consequence that the Bohm trajectories do not cross this plane. In (25), $\delta z(t) = \sqrt{(\delta z_0)^2 + (t\,\delta p/m)^2}$ is the spread in z at time t.

The Bohm-mechanical equation of motion for the trajectory $Z(t)$, *viz.*

$$\frac{\mathrm{d}}{\mathrm{d}t} Z(t) = v(t, Z(t)), \tag{26}$$

is implicitly solved by

$$\int_{-\infty}^{Z(t)} \mathrm{d}z\, \varrho(t, z) = \int_{-\infty}^{Z_0} \mathrm{d}z\, \varrho(0, z), \tag{27}$$

where $Z_0 = Z(0)$ is the initial condition. A final condition could be employed analogously and would, indeed, emphasize the retrodictive nature. In view of

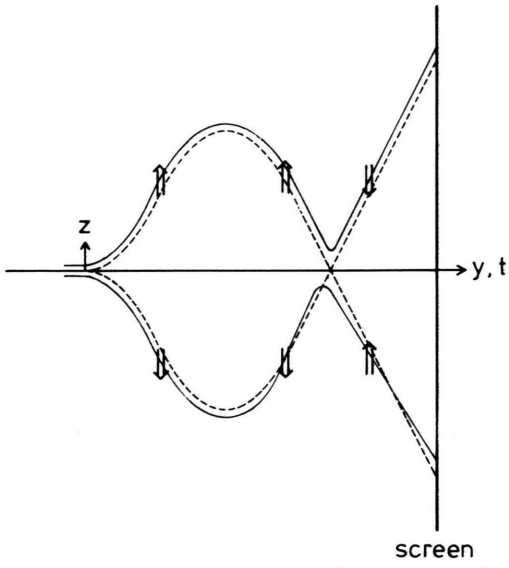

Fig. 5. Bohm trajectories through the incomplete Stern-Gerlach interferometer (magnets not drawn). The dashed curves represent $\pm\Delta z$ of (15); the solid curves are typical Bohm trajectories, which do not cross the $z=0$ plane. The arrows indicate the spin vectors of (29).

(22) with (17), (27) is equivalent to

$$\int_{\Delta z(t)-Z(t)}^{\Delta z(t)+Z(t)} \frac{dz}{\delta z(t)} \exp\left[-\frac{1}{2}\left(\frac{z}{\delta z(t)}\right)^2\right]$$

$$= \int_{-Z_0}^{Z_0} \frac{dz}{\delta z_0} \exp\left[-\frac{1}{2}\left(\frac{z}{\delta z_0}\right)^2\right]. \qquad (28)$$

These integrals can, of course, be evaluated in terms of the error function, but that hardly adds transparence. Note that both integrands are even functions of z, which has the immediate consequence that the sign of $Z(t)$ is that of Z_0, quite independent of the sign of $\Delta z(t)$. So the explicit expression (28) confirms the result of the symmetry consideration: no Bohm trajectory crosses the $z=0$ plane. Further, if Z_0 does not exceed δz_0 by much, as is the most probable situation, and if, in addition, $\Delta z(t)$ is much larger than $\delta z(t)$, signifying a macroscopic separation between ψ_+ and ψ_-, then $|Z(t)|$ does not differ markedly from $|\Delta z(t)|$. Thus, whereas the spatial wave function components $\psi_\pm$ intersect where $\Delta z(t)$ changes sign, each Bohm trajectories first (roughly) follows the center of *one* of the components up to this cross-over region, beyond which they follow the *other*. These statements are illustrated in Figure 5.

The spin vectors indicated in this figure represent what is produced by (6) and (17),

$$\boldsymbol{S}(t) = \left[\cosh\left(\frac{Z(t)\,\Delta z(t)}{(\delta z(t))^2}\right)\right]^{-1} \begin{pmatrix} \cos\varphi(t) \\ \sin\varphi(t) \\ \sinh\left(\dfrac{Z(t)\,\Delta z(t)}{(\delta z(t))^2}\right) \end{pmatrix} \qquad (29)$$

with the effective Larmor angle

$$\varphi(t) = \Phi(t) - \frac{2}{\hbar} Z(t)\left[\Delta p(t) - \frac{t}{m}\left(\frac{\delta p}{\delta z(t)}\right)^2 \Delta z(t)\right]. \qquad (30)$$

Outside the cross-over region, the argument of the hyperbolic functions is large, so that, practically speaking,

$$\boldsymbol{S} = \begin{pmatrix} 0 \\ 0 \\ (\operatorname{sgn} Z_0)\,(\operatorname{sgn}\Delta z) \end{pmatrix} \qquad (31)$$

there. In the cross-over region, the direction of $\boldsymbol{S}$ is reversed, rapidly though continuously.

We now supplement the incomplete Stern-Gerlach interferometer of Figure 4 with two one-bit which-way detectors located where $|\Delta z|$ is largest, that is just after two of the three quarters, see Figure 6. When the detectors are included into the formulation, we have to replace the two-component wave function

$$\Psi = \begin{pmatrix} \psi_+ \\ \psi_- \end{pmatrix} \qquad (32)$$

by a four-component one, i.e.

$$\Psi_{\text{before}} = \begin{pmatrix} \psi_+ \,|\, {}^{\text{no}}_{\text{no}}\rangle \\ \psi_- \,|\, {}^{\text{no}}_{\text{no}}\rangle \end{pmatrix} \qquad (33)$$

at the times before the atom traversed (one of) the detectors, and by

$$\Psi_{\text{after}} = \begin{pmatrix} \psi_+ \,|\, {}^{\text{yes}}_{\text{no}}\rangle \\ \psi_- \,|\, {}^{\text{no}}_{\text{yes}}\rangle \end{pmatrix} \qquad (34)$$

after the transition. Since the which-way detectors have no noticeable influence on the center-of-mass wave functions $\psi_\pm$, both the density ϱ and the current j as well as the velocity field v of (25) remain unaltered. Consequently, the (retrodicted) Bohm trajectories are identical with the ones found without the which-way detectors installed. There is only one difference. The

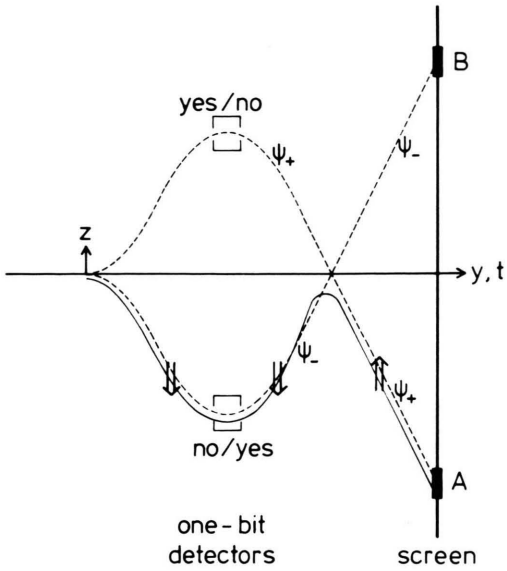

Fig. 6. Incomplete Stern-Gerlach interferometer with one-bit which-way detectors (magnets not drawn). The dashed curves represent $\pm\Delta z(t)$ of (15). The solid curve shows a Bohm trajectory through the *lower* detector, corresponding to an atom that reached the lower region A through the *upper* detector. The arrows indicate the spin vectors of (29) and (35), respectively.

spin vector "after" is not given by (6) and (29) but by

$$\boldsymbol{S}_{\text{after}} = \begin{pmatrix} 0 \\ 0 \\ \operatorname{sgn}(|\psi_+|^2 - |\psi_-|^2) \end{pmatrix} = \begin{pmatrix} 0 \\ 0 \\ (\operatorname{sgn} Z_0)(\operatorname{sgn} \Delta z) \end{pmatrix}, \tag{35}$$

which now applies in the cross-over region, too. Thus, spin-flip now appears to happen instantaneously at the moment when Δz changes sign. For an adherent of Bohmian mechanics this is nothing to worry about, though, because for him spin is a property of the wave function and not carried by the atom itself.

With the which-way detectors in place we can again compare the Bohm trajectory with what is known about the track of the atom. In the lower region A of Figure 6. ψ_- vanishes effectively and only ψ_+ contributes to the density ϱ. Therefore, as implied by (35), if an atom hits the lower screen in region A, it has left a trace in the upper detector. Its Bohm trajectory, in contrast, goes through the lower detector. Likewise, an atom arriving in the upper region B went through the lower detector, but its Bohm trajectory through the upper one. The actual tracks and the Bohm trajectories could not be more at variance than that.

A supporter of Bohmian mechanics woulds insist that the atom went along its Bohm trajectory through one of the detectors, but left its mark in the other one. Thus, he concludes, the which-way detectors do not deserve their name. The usual which-way detection, he declares, is an illusion. But, in arguing this way, is he not putting away with the basics of Bohmian mechanics? For, on the one hand, the retrodicted Bohm trajectories are supposed to be "truly realistic", on the other hand, checking them out is forbidden or, at least, impossible. We conclude: The reality attributed to Bohm trajectories is not physical, it is metaphysical.

A real experiment along these lines appears feasible, as all components of the apparatus have been realized separately; for details consult Appendix A. The purpose of the proposed experiment is to verify the predicted quantum theoretical correlations: Whenever an atom hits the screen in the lower region A, the upper detector says "yes" – and likewise for the upper region B and the lower detector. Since we know that (some of) the retrodicted Bohm trajectories pass through the other detector, this verification suffices to demonstrate the asserted metaphysical character of the Bohm trajectories.

Acknowledgements

BGE and GS are grateful for the hospitality experienced at the Center for Advanced Studies at UNM. This work is partially supported by the Office of Naval Research.

Appendix A

The central instrument needed for the construction of the quantum-optical which-way detector is the micromaser. This [12] consists of a resonator cavity with superconducting walls that enclose a volume of a few cubic centimeters. It is traversed by atoms that are suitably excited prior to entering the cavity. The resonator can be tuned very precisely to transitions between rather neighboring Rydberg states. In the ongoing micromaser experiments, one exemplary transition is between the $63\,p_{3/2}$ and the $61\,d_{5/2}$ states of Rubidium at a frequency of about 21.5 GHz, corresponding to the size of the resonator, which has a cylindrical shape and is about 24 mm both in length and in diameter.

By cooling the cavity to very low temperatures one reduces the number of thermal photons practically to

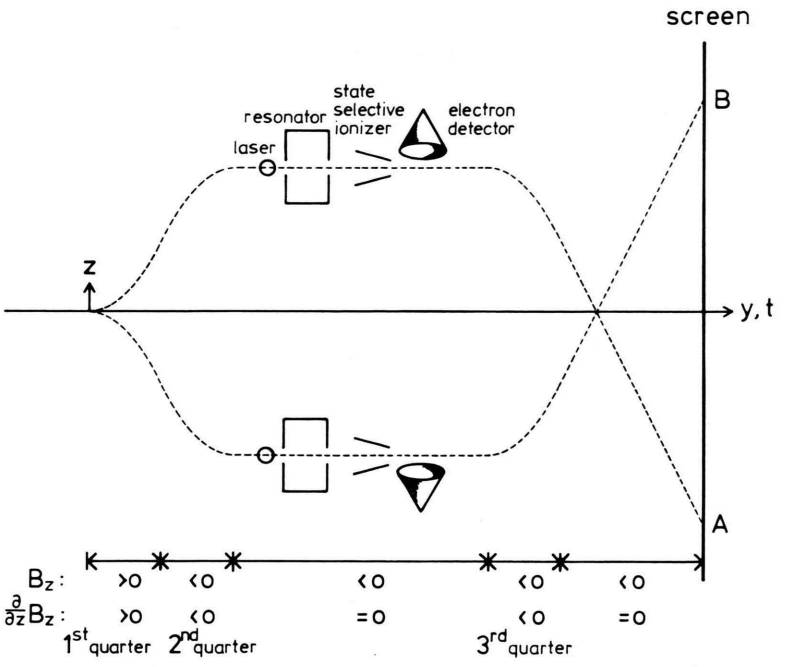

Fig. 7. Schematic set-up of the proposed experimentum crucis. An incomplete Stern-Gerlach interferometer is supplemented – between the second and third quarter – by quantum-optical one-bit which-way detectors consisting of laser beams for the excitation to the Rydberg states, micromaser resonators for storing the tell-tale photons, electrostatic condensors for the state-selective ionization of the Rydberg atoms, and electron detectors. A measurement cycle begins with a laser pulse that excites an atom into the upper Rydberg state. After this atom has been detected on the screen in regions A or B, a second laser pulse excites a reader atom into the lower Rydberg state. This reader atom picks up the tell-tale photon and is detected by the state-selective field ionization.

zero. When an atom, excited to the upper states of the Rydberg transition, enters this empty cavity, it will emit a single microwave photon with virtual certainty, provided that the interaction time is chosen appropriately by controlling the atom's velocity (~ 300 m/s). The emerging atom is then in the lower one or the two relevant Rydberg states. Thus the presence or absence of a photon in the resonator indicates whether an atom went through it or not. The micromaser can, therefore, be used as a one-bit detector sensitive to the passage of a single atom.

The lifetime of the tell-tale photon in the ultracold cavity is as long as a few hundred milliseconds. This is more then enough time for reading off the stored information. For this purpose, a "reader atom" in the lower state of the Rydberg transition is sent through the cavity with the right velocity, so that it absorbs the photon with certainty, if it is there. By state-selective field ionization one can then find out if the emerging reader atom is in the upper or the lower Rydberg state. Thereafter one knows for sure whether a tell-tale photon was stored in the cavity or not.

The interaction of the atom with the microwave cavity field does not appreciably disturb the atom's center-of-mass wave function [13], although the exchange of energy may change the internal atomic state. The center-of-mass motion is most naturally discussed in terms of kinetic and potential energy. In this language, the coupling between the atom and the quantized photon field appears as a very small potential energy whose sign and magnitude depend on the internal atomic and the photonic quantum numbers. The wave function then consists of two components, one exposed to a weak attractive potential and the other to a repulsive one; the dynamical difference between attraction and repulsion effects the internal atomic transition accompanied by the emission or absorption of a photon. After the atom has left the cavity, these potential energies are again zero and the kinetic energy has its initial value. Thus no net momentum is transferred to the atom during the interaction with the cavity field and, accordingly, its center-of-mass wave function is not affected markedly. Perhaps we should also mention that the localized cavity photon does not possess a definite momentum, and therefore the atom-photon interaction calculations cannot be simply carried out on the basis of momentum transfer and the recoil associated with it.

In the incomplete Stern-Gerlach interferometer of Figs. 4–6, the separation of the two partial beams after two of the three quarters can be made so large that enough room is available for the two micromaser resonators, see Figure 7. A sufficiently long stretch with a homogeneous magnetic field between the sec-

ond and third provides the required longitudinal space. The atoms move parallel to the y-axis through this region. The Rb atoms are in their $5s_{1/2}$ ground state when leaving the second quarter with magnetic quantum numbers $m_j = +1/2$ or $m_j = -1/2$, respectively.

Prior to entering either one of the micromaser cavities, a laser beam exites the atom to the $63p_{3/2}$ Rydberg state. It is expedient to use a laser beam propagating along the x-direction and linearly polarized along the z-direction, that is: parallel to the magnetic field. In the π-transitions thus achieved the magnetic quantum number is not changed, so that only the Zeeman levels with $m_j = +1/2$ in the upper partial beam and $m_j = -1/2$ in the lower one get populated. For the same reason, the resonators are oriented such that the polarization of the photon mode is also along the z-direction. Thus, when entering the third quarter of the incomplete Stern-Gerlach interferometer, the Rb atoms are in the $61d_{5/2}$ Rydberg states with $m_j = +1/2$ or $m_j = -1/2$, respectively. Ideally, these atoms are deflected as indicated in Figure 6. In reality, however, the inhomogeneous magnetic field induces transitions to neighboring Rydberg levels with different magnetic properties. As a consequence, the two partial beams acquire a substructure, and a more complicated pattern emerges on the screen. This is not damaging for our purpose because all we need are identifiable regions on the lower/upper half of the screen such that, whenever an atom arrives there, the tell-tale photon is found in the upper/lower resonator. These regions are surely there.

To maintain the essential symmetry of the set-up the two laser beams in Fig. 7 have to be *equivalent* partial beams produced by sending the output of a single laser through a beam splitter. The laser frequency can be so adjusted that either the upper or the lower one of the two relevant Rydberg states is excited. In each measurement cycle, the laser is first tuned to the upper Rydberg state and switched on for a period so short that one atom at most is excited. After this atom has reached the screen, the laser is again activated for a short while, this time tuned to the lower Rydberg state. The second Rydberg atom possibly thus produced will absorb the tell-tale photon left behind by the first atom, thereby reading-off the which-way information stored in the respective resonator. The "reader atom" is then in the upper Rydberg state. It is ionized in an inhomogeneous static electric field whose strength is such that it cannot ionize atoms in the lower Rydberg state. The electron stripped off the reader atom is then detected. After waiting long enough to ensure that an unnoticed tell-tale photon has faded away, the next cycle is started. Each cycle in which one of the electron detectors responds supplies us with one atom whose track through the incomplete Stern-Gerlach interferometer is known.

Appendix B

The yes/no label attached to the quantum-optical which-way detectors of Appendix A refers to the presence or absence of one photon only. The photon modes in question can be regarded as harmonic oscillators which are either in their respective ground states ("no") or first excited states ("yes"). Rather than using discrete photon numbers, one could thus employ (dimensionless) position variables, q_1 and q_2, and the corresponding harmonic oscillator wave functions to represent the state of the system. In Bohmian mechanics the two harmonic oscillators are also subject to a dynamical evolution, although their waves remain in their ground or first excited state, respectively.

The four-component wave function $\Psi(t, z)$ of (34) is then replaced by a two-component one, *viz.*

$$\Psi(t, z; q_1, q_2) = \begin{pmatrix} \Psi_+ \\ \Psi_- \end{pmatrix}$$

$$= \sqrt{2/\pi}\, \exp(-\tfrac{1}{2} q_1^2 - \tfrac{1}{2} q_2^2) \begin{pmatrix} q_1\, \psi_+(t, z) \\ q_2\, \psi_-(t, z) \end{pmatrix} \qquad (36)$$

with $\psi_\pm(t, z)$ from (17). For notational simplicity we drop the subscript "after". The probability density is now

$$\varrho(t, z; q_1, q_2) = |\Psi_+|^2 + |\Psi_-|^2 \qquad (37)$$

$$= \frac{2}{\pi} \exp(-q_1^2 - q_2^2)\, [q_1^2 |\psi_+(z)|^2 + q_2^2 |\psi_-(t, z)|^2]$$

and the current components are given by

$$j_z(t, z; q_1, q_2) = \frac{\hbar}{m} \operatorname{Im} \left\{ \Psi_+^* \frac{\partial}{\partial z} \Psi_+ + \Psi_-^* \frac{\partial}{\partial z} \Psi_- \right\}$$

$$= \frac{2}{\pi} \frac{\hbar}{m} \exp(-q_1^2 - q_2^2) \left[q_1^2 \operatorname{Im} \left\{ \psi_+^* \frac{\partial}{\partial z} \psi_+ \right\} \right. \qquad (38)$$

$$\left. + q_2^2 \operatorname{Im} \left\{ \psi_-^* \frac{\partial}{\partial z} \psi_- \right\} \right]$$

as well as

$$j_1(t, z; q_1, q_2) = \omega \operatorname{Im}\left\{\Psi_+^* \frac{\partial}{\partial q_1} \Psi_+ + \Psi_-^* \frac{\partial}{\partial q_1} \Psi_-\right\} = 0,$$
$$j_2(t, z; q_1, q_2) = \omega \operatorname{Im}\left\{\Psi_+^* \frac{\partial}{\partial q_2} \Psi_+ + \Psi_-^* \frac{\partial}{\partial q_2} \Psi_-\right\} = 0, \tag{39}$$

where ω denotes the common natural frequency of the oscillators. The velocity fields

$$v_1 = j_1/\varrho, \quad v_2 = j_2/\varrho, \tag{40}$$

for the $q_{1,2}$ motions, vanish so that the oscillators do not actually move. The velocity field for the atom's z-motion,

$$v_z(t, z; q_1, q_2) = j_z/\varrho \tag{41}$$
$$= t\, z\left(\frac{\delta p}{m\, \delta z(t)}\right)^2 + \left[\frac{\Delta p(t)}{m} - t\, \Delta z(t)\left(\frac{\delta p}{m\, \delta z(t)}\right)^2\right] \cdot \frac{q_1^2 \exp\left(\frac{z\, \Delta z(t)}{(\delta z(t))^2}\right) - q_2^2 \exp\left(-\frac{z\, \Delta z(t)}{(\delta z(t))^2}\right)}{q_1^2 \exp\left(\frac{z\, \Delta z(t)}{(\delta z(t))^2}\right) + q_2^2 \exp\left(-\frac{z\, \Delta z(t)}{(\delta z(t))^2}\right)}$$

is different from (25) unless $q_1^2 = q_2^2$. Consequently, the implied trajectories $Z(t)$ are not the ones generated by (25). In particular, the new trajectories *may* cross the $z=0$ plane, and some of them do so.

The Bohm trajectories stay now in the three-dimensional z, q_1, q_2-space: $Z(t), Q_1(t), Q_2(t)$. They are determined by

$$\frac{\mathrm{d}}{\mathrm{d}t} Z = v_z(t, Z; Q_1, Q_2),$$
$$\frac{\mathrm{d}}{\mathrm{d}t} Q_1 = v_1(t, Z; Q_1, Q_2), \tag{42}$$
$$\frac{\mathrm{d}}{\mathrm{d}t} Q_2 = v_2(t, Z; Q_1, Q_2).$$

In view of $v_1 = v_2 = 0$ there is a set of $Z(t)$ trajectories to each pair of initial Q_1, Q_2 values, and two trajectories from the same set do not intersect in the t, z plane. Therefore, to calculate the probability that the atomic $Z(t)$ trajectory crosses the $z=0$ plane we first compare, for given Q_1 and Q_2, the probabilities for finding the atom below the $z=0$ plane at the initial and final times t_i and t_f, and then integrate over all Q_1 and Q_2 values. The probability for crossing is thus

$$P_{\text{crossing}} = \int_{-\infty}^{\infty} \mathrm{d}Q_1 \int_{-\infty}^{\infty} \mathrm{d}Q_2 \left| \int_{-\infty}^{0} \mathrm{d}z\, [\varrho(t_\mathrm{i}, z; Q_1, Q_2) - \varrho(t_\mathrm{f}, z; Q_1, Q_2)] \right| = \sqrt{2/\pi^3} \left| \int_{(\Delta z/\delta z)_\mathrm{f}}^{(\Delta z/\delta z)_\mathrm{i}} \mathrm{d}s\, e^{-\frac{1}{2}s^2} \right|. \tag{43}$$

This is to be applied to the situation in which $\Delta z/\delta z \gg 1$ initially and $-\Delta z/\delta z \gg 1$ finally. Then the s integral equals $\sqrt{2\pi}$ and the crossing probability is $2/\pi = 64\%$. The remaining 36% of the atomic trajectories do not cross the $z=0$ plane, so they do not pass through the same detector as the atom's track.

The spin vector associated with the Z, Q_1, Q_2 trajectory is

$$\boldsymbol{S} = \left[Q_1^2 \exp\left(\frac{Z\, \Delta z}{(\delta z)^2}\right) + Q_2^2 \exp\left(-\frac{Z\, \Delta z}{(\delta z)^2}\right)\right]^{-1} \cdot \begin{pmatrix} 2 Q_1 Q_2 \cos\varphi \\ 2 Q_1 Q_2 \sin\varphi \\ Q_1^2 \exp\left(\frac{Z\, \Delta z}{(\delta z)^2}\right) - Q_2^2 \exp\left(-\frac{Z\, \Delta z}{(\delta z)^2}\right) \end{pmatrix}, \tag{44}$$

which is different from both (35) and (29). It has more in common with the latter, which is contained as the symmetric $Q_1 = Q_2$ case. Along those $Z(t)$ trajectories that do not cross the $z=0$ plane, the direction of $\boldsymbol{S}(t)$ is reversed in the cross-over region, rapidly though continuously. The instantaneous spin flip observed for (35) would require $Q_1 = 0$ or $Q_2 = 0$, in which situation practically all $Z(t)$ trajectories cross the $z=0$ plane and $\boldsymbol{S}(t)$ is time independent. Accordingly, that instantaneous spin flip does not occur.

For the double-slit interferometer with which-way detectors considered by Bell [6], the Z, Q_1, Q_2 trajectories are more complicated because Q_1 and Q_2 possess a genuine time dependence. Analogously to (36), we replace the two-component wave function (9) by the single function

$$\psi(t, \boldsymbol{r}; q_1, q_2) \tag{45}$$
$$= \sqrt{2/\pi} \exp(-\tfrac{1}{2} q_1^2 - \tfrac{1}{2} q_2^2)\, [q_1 \psi_>(t, \boldsymbol{r}) + q_2 \psi_<(t, \boldsymbol{r})].$$

There are now interference terms in the resulting probability density

$$\varrho(t, \boldsymbol{r}; q_1, q_2) = |\psi|^2 = \frac{2}{\pi} \exp(-q_1^2 - q_2^2) \tag{46}$$
$$\cdot\, [q_1^2 |\psi_>|^2 + q_2^2 |\psi_<|^2 + 2 q_1 q_2 \operatorname{Re}\{\psi_>^* \psi_<\}]$$

as well as in the currents and Bohm velocity fields

$$\boldsymbol{j}(t,\boldsymbol{r};q_1,q_2)=\varrho\,\boldsymbol{v}(t,\boldsymbol{r};q_1,q_2)=\frac{\hbar}{m}\,\mathrm{Im}\{\psi^*\nabla\psi\}$$
$$=\frac{2}{\pi}\frac{\hbar}{m}\exp(-q_1^2-q_2^2)$$
$$\cdot\,\mathrm{Im}\{q_1^2\psi_>^*\nabla\psi_>+q_2^2\psi_<^*\nabla\psi_<+q_1q_2(\psi_<^*\nabla\psi_<+\psi_<^*\nabla\psi_>)\},$$

$$j_1(t,\boldsymbol{r};q_1,q_2)=\varrho\,v_1(t,\boldsymbol{r};q_1,q_2)=\omega\,\mathrm{Im}\left\{\psi^*\frac{\partial}{\partial q_1}\psi\right\}$$
$$=\omega\frac{2}{\pi}\exp(-q_1^2-q_2^2)\,q_2\,\mathrm{Im}\{\psi_<^*\psi_>\},\tag{47}$$

$$j_2(t,\boldsymbol{r};q_1,q_2)=\varrho\,v_2(t,\boldsymbol{r};q_1,q_2)=\omega\,\mathrm{Im}\left\{\psi^*\frac{\partial}{\partial q_2}\psi\right\}$$
$$=\omega\frac{2}{\pi}\exp(-q_1^2-q_2^2)\,q_1\,\mathrm{Im}\{\psi_>^*\psi_<\}.$$

In contrast to (39), the velocities for the $q_{1,2}$ motions do not vanish here. But there is still a constant of motion, namely $Q_1^2+Q_2^2$, as implied by

$$q_1j_1+q_2j_2=0\,.\tag{48}$$

This invites the use of polar coordinates in the q_1,q_2-plane for the parameterization of $Q_1(t)$ and $Q_2(t)$,

$$Q_1(t)=Q\cos\vartheta(t),\quad Q_2(t)=Q\sin\vartheta(t),\tag{49}$$

where $Q>0$ is time independent.

The Bohm mechanical time dependence of $\vartheta(t)$ and of the atom trajectory $\boldsymbol{R}(t)$ are determined by

$$\frac{\mathrm{d}}{\mathrm{d}t}\boldsymbol{R}=\boldsymbol{v}(t,\boldsymbol{R};Q\cos\vartheta,Q\sin\vartheta)\,,\tag{50}$$

where the right-hand side is actually independent of Q, and

$$\frac{\mathrm{d}}{\mathrm{d}t}\vartheta=\frac{\omega}{Q^2}\,\frac{\mathrm{Im}\{\psi_>^*(t,\boldsymbol{R})\,\psi_<(t,\boldsymbol{R})\}}{|\psi_>(t,\boldsymbol{R})\cos\vartheta+\psi_<(t,\boldsymbol{R})\sin\vartheta|^2}\,.\tag{51}$$

After restricting the atomic motion to the z-direction for simplicity and modeling the double-slit wave functions $\psi_>$ and $\psi_<$ by ψ_+ and ψ_- from (17) with $\phi\equiv 0$, we have studied these equations numerically for the relevant period between $t=3\,T_0$ and $t=4\,T_0$. When the same order of magnitude was chosen for the time scales of the evolution of $Z(t)$ and $\vartheta(t)$, as expressed by $\omega\,T_0\cong 1\cdots 10$, we found that the Bohm trajectories depend very sensitively on the initial values of Z, ϑ, and Q. We note that this range of oscillator frequencies is, of course, much smaller than is physically reasonable. Since an analysis like the one that produced (43) above appears impossible here, we have resorted to computing a few hundred trajectories with their initial values selected at random. About 20% of them do not cross ther $z=0$ plane. So here, too, a substantial fraction of the atomic Bohm trajectories do not pass through the same detector as the atom's track.

When, in contrast, very different time scales were chosen, such as by the physically reasonable value of $\omega\,T_0=10^5$, we did not find a single trajectory that crosses the $z=0$ plane. Here, very few Bohm trajectories, at best, pass through the same detector as the atom's track. This behavior results from the different frequencies. For, the angle $\vartheta(t)$ grows so fast that $\sin\vartheta$ and $\cos\vartheta$ in (50) oscillate extremely rapidly, so that $\boldsymbol{v}$ of (50) can be effectively replaced by its ϑ-average,

$$\frac{\mathrm{d}}{\mathrm{d}t}\boldsymbol{R}=\boldsymbol{v}_{\mathrm{av}}(t,\boldsymbol{R})=\int\limits_{(2\pi)}\frac{\mathrm{d}\vartheta}{2\pi}\,\boldsymbol{v}(t,\boldsymbol{R};Q\cos\vartheta,Q\sin\vartheta)\,.\tag{52}$$

The resulting averaged velocity field $\boldsymbol{v}_{\mathrm{av}}(t,\boldsymbol{r})$ has the required symmetry property: its z-component changes sign under the reflection $\boldsymbol{r}=(x,y,z)\to(x,y,-z)$. Consequently, the Bohm trajectories generated by $\boldsymbol{v}_{\mathrm{av}}$ must stay on one side of the $z=0$ plane.

[1] D. Bohm, Phys. Rev. **85,** 166 (1952) and **85,** 180 (1952); both reprinted in: Quantum Theory and Measurement (J. A. Wheeler and W. H. Zurek, eds.), Princeton University Press 1983.

[2] D. Bohm and B. J. Hiley, Found. Phys. **5,** 93 (1975).

[3] D. Bohm, J. Hiley, and P. N. Kaloyerou, Phys. Rep. **144,** 321 (1987).

[4] D. Bohm, Quantum Theory, Prentice-Hall, Englewood Cliffs 1951.

[5] M. O. Scully, B.-G. Englert, and J. Schwinger, Phys. Rev. A **40,** 1775 (1989).

[6] J. S. Bell, Int. J. Quant. Chem. **14,** 155 (1980); reprinted in: Speakable and unspeakable in quantum mechanics, Cambridge University Press 1987.

[7] D. Dürr, S. Goldstein, and N. Zanghi, J. Stat. Phys. **67,** 843 (1992).

[8] C. Philippidies, C. Dewdney, and B. J. Hiley, Nuovo Cim. **52B,** 15 (1979).

[9] M. O. Scully, B.-G. Englert, and H. Walther, Nature London **351,** 111 (1991).

[10] J. Schwinger, M. O. Scully, and B.-G. Englert, Z. Phys. D **10,** 135 (1988).

[11] B.-G. Englert, J. Schwinger, and M. O. Scully, Found Phys. **18,** 1045 (1988).

[12] For a review of the Garching micromaser work see: G. Rempe, M. O. Scully, and H. Walther, Physica Scripta **T34,** 5 (1991).

[13] B.-G. Englert, J. Schwinger, and M. O. Scully, in: New Frontiers in Quantum Electrodynamics (A. O. Barut, ed.) Plenum, New York 1990, pp. 513–519.